ISSN 1070-3284, Russian Journal of Coordination Chemistry, 2014, Vol. 40, No. 8, pp. 523–530. © Pleiades Publishing, Ltd., 2014.
Original Russian Text © S.I. Levchenkov, I.N. Shcherbakov, L.D. Popov, V.G. Vlasenko, K.Yu. Suponitskii, A.A. Tsaturyan, V.V. Lukov, V.A. Kogan, 2014, published in Koordinatsionnaya Khimiya, 2014, Vol. 40, No. 8, pp. 451–459.

Influence of the Bridging Coordination of DMSO on the Exchange Interaction Character in the Binuclear Copper(II) Complex with the Nonsymmetrical Exchange Fragment

S. I. Levchenkov[a, *], I. N. Shcherbakov[b], L. D. Popov[b], V. G. Vlasenko[b], K. Yu. Suponitskii[c], A. A. Tsaturyan[b], V. V. Lukov[b], and V. A. Kogan[b]

[a] *Southern Scientific Center, Russian Academy of Sciences, Rostov-on-Don, Russia*
[b] *Southern Federal University, Rostov-on-Don, 344104 Russia*
[c] *Nesmeyanov Institute of Organoelement Compounds, Russian Academy of Sciences, ul. Vavilova 28, Moscow, 119991 Russia*
**e-mail: s.levchenkov@gmail.com*

Received November 28, 2013

Abstract—The binuclear copper(II) complex $[Cu_2L(CH_3COO)]$ (**I**), where L^{3-} is the azomethine trianion based on 3-methyl-4-formyl-1-phenylpyrazol-5-one and 1,3-diaminopropan-2-ol, and its DMSO adduct (**II**) in which the DMSO molecule acts as an additional bridging ligand are synthesized. The structure of complex **II** is determined by X-ray diffraction analysis, and the structure parameters of the coordination unit of complex **I** are determined by EXAFS spectroscopy. The μ_2-coordination of the DMSO molecule in compound **II** results in a change in the sign of the exchange interaction parameter. In complex **I**, the antiferromagnetic exchange interaction ($2J = -169$ cm^{-1}) occurs between the copper(II) ions. The exchange interaction of the ferromagnetic type ($2J = 174$ cm^{-1}) is observed in complex **II**. The quantum-chemical calculations of the magnetic exchange parameters by the density functional theory method show that the role of the DMSO molecule as a switch of the exchange interaction character is exclusively the stabilization of the "broken" conformation of the metallocycles.

DOI: 10.1134/S1070328414080041

INTRODUCTION

Bis(azomethines) are the condensation products of polyfunctional aldehydes with 1,3-diaminopropan-2-ol and classical binucleating ligand systems [1–5]. They are characterized by the formation of binuclear complexes in which the alkoxyl oxygen atom is one of the bridges connecting two metal ions, whereas the second bridge is the exogenic bridging ligand that can be presented by carboxylic acid residues, phosphate ion derivatives, and pyrazolate, azaindolate, or purinate ions [6–11]. The complexes with the nonsymmetrical exchange fragment are convenient models for the study of the main factors determining the character and magnitude of exchange interactions between paramagnetic centers [5].

The results of the synthesis, physicochemical study, and quantum-chemical simulation of the binuclear copper(II) complex $[Cu_2L(CH_3COO)]$ (**I**), where L^{3-} is the bis(azomethine) anion, and its DMSO solvate (**II**) demonstrating different magnetic properties are presented in this report.

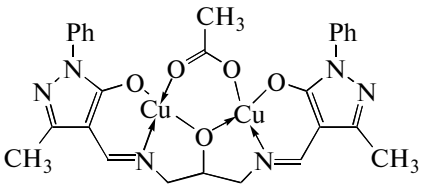

I

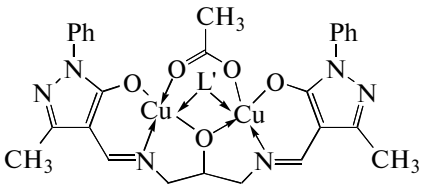

II, L' = DMSO

Table 1. Crystallographic data and the experimental and refinement details for complex **II**

Parameter	Value
FW	797.87
Crystal size, mm	$0.45 \times 0.35 \times 0.30$
Temperature, K	100(2)
Crystal system	Monoclinic
Space group	$P2_1/c$
a, Å	20.028(2)
b, Å	7.8496(8)
c, Å	21.608(2)
β, deg	93.786(2)
V, Å^3	3389.7(6)
Z	4
ρ_{calcd}, g/cm^3	1.563
μ, mm^{-1}	1.434
$F(000)$	1648
$2\theta_{max}$, deg	52
Number of measured reflections	23713
Number of independent reflections	6585
Number of reflections with $I > 2\sigma(I)$	5428
Ranges of reflection indices	$-24 < h < 22$, $-9 < k < 9$, $-26 < l < 26$
Number of refined parameters	439
R_1 ($I > 2\sigma(I)$)	0.0657
wR_2 (all reflections)	0.1396
Goodness-of-fit for (all reflections)	1.027
$\Delta\rho_{max}/\Delta\rho_{min}$, e Å^{-3}	0.906/−1.164

EXPERIMENTAL

Commercially available reagents were used as the starting compounds. The solvents were purified and dried according to standard procedures.

IR spectra were recorded on a Varian Scimitar 1000 FT-IR instrument in the range from 400 to 4000 cm^{-1}, and the samples were prepared as suspensions in Nujol. Elemental analysis was carried out on a PerkinElmer 240C instrument at the Laboratory of Microanalysis of the Southern Federal University. Thermogravimetry was carried out on a PerkinElmer Diamond TG/DTA instrument, and the samples were heated to 650°C with a rate of 10 deg/min. The magnetic susceptibility was determined on a Quantum Design SQUID magnetometer in the temperature range from 2 to 300 K in a magnetic field of 1 kOe.

Azomethine H_3L was synthesized according to a described procedure [12].

Synthesis of complex I. A hot solution of copper(II) acetate (2 mmol) in methanol (10 mL) was added to a hot solution of H_3L (1 mmol) in methanol (10 mL). The resulting solution was refluxed for 1 h. The precipitate was filtered off, washed with hot methanol, and dried in vacuo. The yield was 0.37 g (57%), mp > 250°C.

For $C_{27}H_{26}N_6O_5Cu_2$

anal. calcd., %: C, 50.54; H, 4.08; N, 13.10; Cu, 19.81.
Found, %: C, 50.20; H, 4.19; N, 13.27; Cu, 20.03.

IR, ν, cm^{-1}: 1632, 1595 ν(C=N).

Complex II was obtained by the recrystallization of compound **I** from DMSO, mp > 250°C.

For $C_{31}H_{38}N_6O_7S_2Cu_2$

anal. calcd., %: C, 50.40; H, 4.46; N, 9.80; Cu, 14.81.
Found, %: C, 50.46; H, 4.57; N, 9.74; Cu, 14.92.

IR, ν, cm^{-1}: 1635, 1596 ν(C=N).

The X-ray diffraction analysis for complex **II** was carried out on a Bruker SMART 1000 CCD diffractometer (MoK_α, λ = 0.71073 Å, graphite monochromator). The initial array of measured intensities was processed using the SAINT [13] and SADABS programs [14]. The structure was solved by a direct method and refined by full-matrix least squares in the anisotropic approximation for non-hydrogen atoms for F^2_{hkl}. Hydrogen atoms were placed in the geometrically calculated positions and refined by the riding model ($U_{iso}(H) = nU_{iso}(C)$, where $n = 1.5$ for the carbon atoms of the methyl groups and $n = 1.2$ for other C atoms). All calculations were performed using the SHELXTL program package [15]. The experimental characteristics and crystallographic data are presented in Table 1. Selected interatomic distances and bond angles are given in Table 2. The coordinates of atoms and other structure parameters for complex **II** were deposited with the Cambridge Crystallographic Data Centre (no. 836304; deposit@ccdc.cam.ac.uk or http://www.ccdc.cam.ac.uk/data_request/cif).

The copper K-edge X-ray absorption spectra of complex **I** were obtained in the transmission mode on an EXAFS spectrometer of the K1.3b station "Structural Materials Science" at the Kurchatov Synchrotron Center. The energy of an electron beam used as an X-ray synchrotron radiation source was 2.5 GeV at a current of 80–100 mA. A Si(111) two-crystal monochromator was used for the monochromatization of the X-ray radiation. The obtained spectra were processed using standard procedures of background picking out, normalizing to the K-edge jump, and isolating the atomic absorption μ_0 [16], after which the obtained EXAFS (χ) spectra were Fourier-transformed in the range of wave vectors of photoelectrons k from 2.5 to 13.0 Å^{-1} with the weight function k^3. The threshold ionization energy E_0 was chosen by the value of the first derivative maximum of the K edge and fur-

Table 2. Selected interatomic distances and bond angles in the coordination polyhedra of the copper atoms in the structure of complex **II**

Bond	*d*, Å	Bond	*d*, Å
Cu(1)–O(2)	1.928(4)	Cu(2)–O(3)	1.946(4)
Cu(1)–N(1)	1.937(5)	Cu(2)–N(4)	1.945(4)
Cu(1)–O(1)	1.938(4)	Cu(2)–O(1)	1.947(4)
Cu(1)–O(5)	1.976(4)	Cu(2)–O(6)	1.954(4)
Cu(1)–O(4)	2.373(4)	Cu(2)–O(4)	2.433(4)
Angle	ω, deg	Angle	ω, deg
O(2)Cu(1)N(1)	96.13(18)	O(3)Cu(2)N(4)	95.94(18)
O(2)Cu(1)O(1)	177.28(17)	O(3)Cu(2)O(1)	174.15(17)
N(1)Cu(1)O(1)	84.10(18)	N(4)Cu(2)O(1)	84.68(18)
O(2)Cu(1)O(5)	89.59(16)	O(3)Cu(2)O(6)	87.63(16)
N(1)Cu(1)O(5)	157.85(19)	N(4)Cu(2)O(6)	174.74(19)
O(1)Cu(1)O(5)	91.20(16)	O(1)Cu(2)O(6)	91.38(16)
O(2)Cu(1)O(4)	91.85(15)	O(3)Cu(2)O(4)	102.03(15)
N(1)Cu(1)O(4)	113.80(18)	N(4)Cu(2)O(4)	91.28(17)
O(1)Cu(1)O(4)	85.59(15)	O(1)Cu(2)O(4)	83.75(15)
O(5)Cu(1)O(4)	87.29(15)	O(6)Cu(2)O(4)	91.75(15)

Table 3. Structural data for the local atomic environment of the copper atom in complex **I** obtained from the multisphere fitting of the EXAFS data*

N	*R*, Å	σ^2, Å^2	Atom	*Q*, %
2	1.91	0.0035	N/O	1.0
2	2.00	0.0035	N/O	
1	3.51	0.0050	Cu	

* *R* are interatomic distances, *N* is the coordination number, σ^2 is the Debye–Waller factor, and *Q* is the goodness-of-fit function.

ther was varied during fitting. The structure parameters of the local environment of the copper atoms were determined by the nonlinear fitting of the parameters of the corresponding coordination spheres when comparing the calculated EXAFS signal and the signal picked out from the full EXAFS spectrum by the Fourier filtration of the corresponding Fourier transformant modules (FTM). The fitting was performed using the IFFEFIT-1.2.11 program package [17]. The scattering phases and amplitudes of the photoelectron waves necessary for the construction of the model spectrum were calculated by the FEFF7 program [18] using the atomic coordinates of model compounds. The copper(II) complexes with a similar local structure for which the X-ray diffraction data are known were chosen as model compounds. The goodness-of-fit function *Q*, which was minimized when finding the structure parameters of the nearest environment, was calculated by the formula

$$Q = \frac{\sum\left[k\chi_{\exp}(k) - k\chi_{\text{th}}(k)\right]^2}{\sum\left[k\chi_{\exp}(k)\right]^2} \times 100\%. \qquad (1)$$

The structural data for the local atomic environment of the copper atom in complex **I** obtained from the EXAFS data are listed in Table 3.

Quantum-chemical calculations were performed in the framework of the density functional theory (DFT) using the B3LYP hybrid exchange correlation functional [19, 20]. The earlier approved [21] procedure based on the known "broken symmetry" approach [22–25] was used for the calculation of the exchange parameters 2*J*. The geometry was optimized over all geometric parameters without symmetry restraints. The 6-311G(*d*) split-valence basis set was employed. The calculations were performed at the WSD Cluster at SFedU using the Gaussian 03 program [26]. The Chemcraft program was used to prepare data and presentation graphics and to visualize

Table 4. Energies of triplet states (*HS*) and "broken symmetry" states (*BS*), calculated exchange parameters 2*J*, bond angles α at the alkoxide bridging atom, dihedral angles θ between the coordination planes, and Cu–Cu distances in complexes **I** and **II** according to the calculation

Complex	Conformation	α, deg	θ, deg	*d*(Cu···Cu), Å	Total state energy, aeu		$2J_{\text{calcd}}$, cm^{-1}
					HS	*BS*	
Fixed geometry							
I*	δλ	104.7	61.92	3.078	−5030.2143047	−5030.2138927	180
II	δλ				−5583.4075163	−5583.4071193	174
Optimized geometry							
I	λλ	129.9	28.94	3.514	−5030.6662675	−5030.6666033	−146
	δλ	114.7	49.20	3.273	−5030.6643808	−5030.6642226	69
II	λλ	115.4	56.65	3.284	−5583.9437462	−5583.9434728	120
	δλ	106.2	59.42	3.131	−5583.9483603	−5583.9480119	153

* The coordinates of atoms are taken from the X-ray diffraction data for complex **II**; the DMSO molecule is removed.

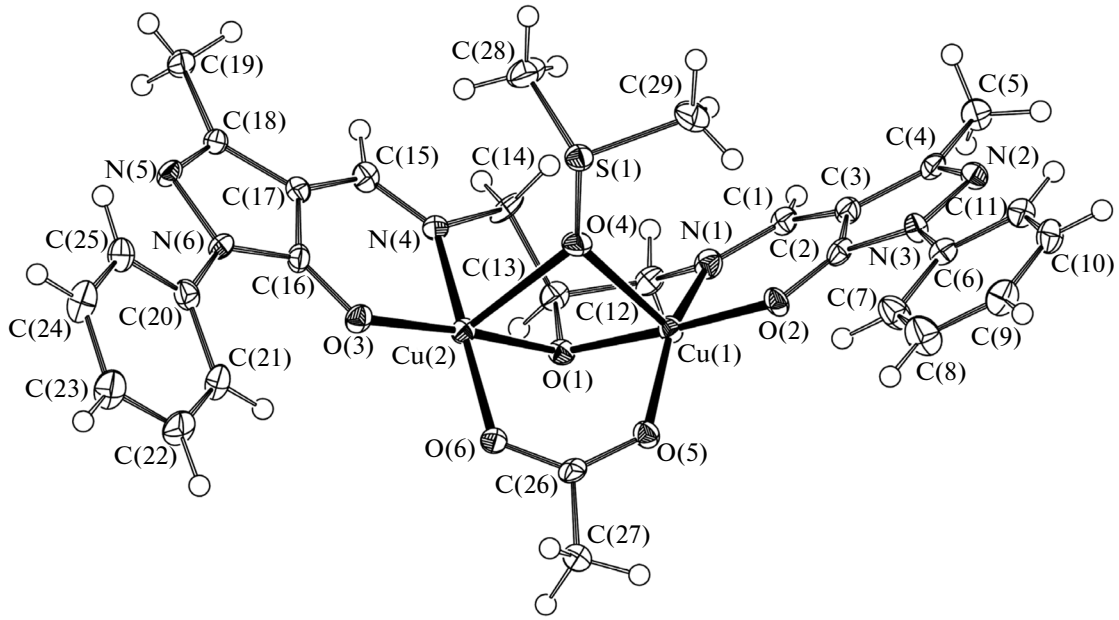

Fig. 1. Structure of complex **II** in the representation of atoms by ellipsoids of thermal displacements with 50% probability.

calculation results [27]. The energies of triplet and "broken symmetry" states and the calculated and experimental exchange parameters 2*J* for complexes **I** and **II** are presented in Table 4.

RESULTS AND DISCUSSION

The compositions and structures of the complexes were established from the data of elemental analysis, IR and EXAFS spectroscopy, thermogravimetry and differential thermal analysis, and magnetochemistry. The structure of complex **II** was determined by X-ray diffraction analysis.

The IR spectroscopy data confirm that azomethine H_3L is coordinated in the pentadentate mode in the triply deprotonated form in all cases [12]. The derivatogram of complex **I** exhibits the mass loss and endotherms in the region below 290°C, indicating the absence of solvent molecules in the composition of the complex [28]. The derivatogram of complex **II** in the range from 100 to 120°C exhibits a sharp mass loss (–17.8% corresponding to two DMSO molecules), after which the weight of the samples remains unchanged to a temperature of 300°C at which thermal decomposition occurs.

Complex **II** (Fig. 1) shows a substantial distortion of the structure of the binuclear molecule: the exogenic acetate bridge fixes the bent conformation of the azomethine ligand. This distortion is additionally favored by the bidentate-bridging coordination of the DMSO molecule that is rarely met in similar complexes. The crystal structure of complex **II** includes an additional DMSO molecule that is not coordinated to the copper ions.

In complex **II**, the copper atoms are bound through three bridges: the alkoxide O(1) atom, the O(4) atom of the coordinated DMSO molecule, and the O(5)–C(26)–O(6) carboxylate group. The coordination polyhedron of both copper atoms is an extended square pyramid (4 + 1) with common atoms: axial O(1) and apical O(4).

Both six-membered chelate cycles in complex **II** are nearly planar, and all atoms lie in the plane of the pyrazole cycle. The deviation of the copper atoms from the plane determined by nine atoms of the chelate and pyrazole cycles is 0.024(4) and 0.038(4) Å for Cu(1) and Cu(2), respectively. The dihedral angle between the planes is 60.22(14)°.

The bond angle Cu(1)O(1)Cu(2) is 104.7(2)°. The alkoxide bridging O(1) atom is strongly pyramidized, and the sum of bond angles at this atom is 329.9°.

As a whole, the molecule of complex **II** is generally roof-shaped, and the θ dihedral angle between the Cu(1)O(1)C(13) and Cu(2)O(1)C(13) planes usually used as a quantitative measure of this distortion is 61.92°.

The bimetallic fragment is distorted because of different conformations of the five-membered metallocycles separated by the alkoxo group [29]. The cycle including the Cu(1) atom has a twist conformation relatively to the C(12)–C(13) bond, and the cycle including the Cu(2) atom has an envelope conformation, which "valve" is formed by the C(14) atom shifted from the plane of other atoms by 0.434(4) Å. As a result, methylene atoms C(12) and C(14) are on opposite sides of the C(13)–O(1) bond common for both cycles and the distorted (δλ [29]) conformation of the binuclear complex are observed.

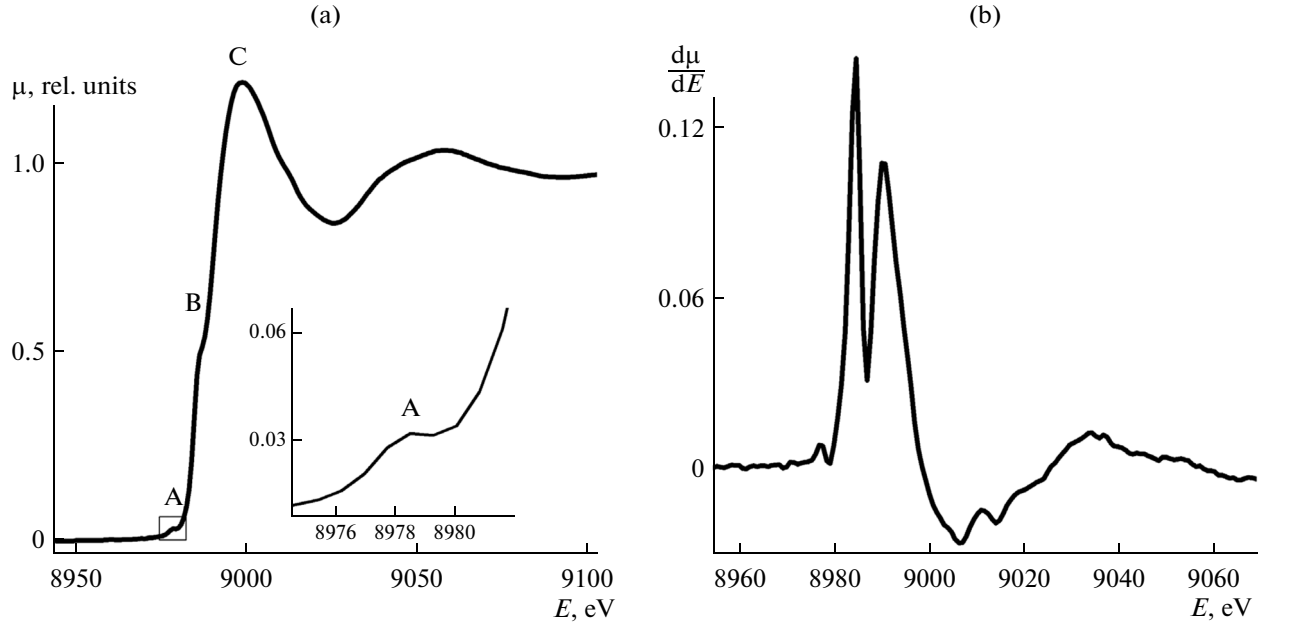

Fig. 2. (a) XANES Cu *K*-edge X-ray absorption spectrum of complex **I** (inset: pre-edge structure) and (b) its first derivative.

The Cu···Cu distance in complex **II** (3.0780(9) Å) is substantially shorter than those in the most part of the earlier described acetate-bridged binuclear copper(II) complexes with bis(azomethines) based on 1,3-diaminopropan-2-ol with the structure close to planar. The methylene atoms in these complexes are arranged at one side from the alkoxo group (symmetrical, or λλ conformation [29]), and the Cu–Cu distance ranges from 3.3 to 3.5 Å [5, 11, 30–34].

The distorted structure similar to that of complex **II** is typical of a series of acetate-bridged copper(II) complexes with bis(azomethines) based on the derivatives of salicylaldehyde and 1,3-diaminopropan-2-ol [11, 34–36]. In all cases, the bridging coordination of the solvent molecule (DMF or DMSO) is observed. A substantial distortion of the binuclear molecules takes place also for a series of the tetranuclear complexes with ligands of this type in which two binuclear fragments are connected due to the bridging function of the dicarboxylic acid residue. In all cases, the bridging coordination of the solvent molecule is observed [37–39]. The single example where the complex of a similar type has a distorted structure without an additional coordination of the solvent is the copper(II) complex with *N,N*-bis(salicylidene)-1,3-diaminopropan-2-ol and the exogenic formate bridge [29].

Complex **I** was studied by X-ray absorption near-edge structure (XANES) spectroscopy to establish the local atomic environment of the copper(II) ions. The XANES Cu *K*-edge X-ray absorption spectrum of complex **I** and its first derivative are presented in Fig 2. The low-intensity pre-edge structure A (8978 eV) assigned to the $1s \rightarrow 3d$ electronic transition indicates the low-symmetry environment of the copper ions in the oxidation state 2+ [40]. The fine XANES structure of the complexes in the region of the edge and above the absorption edge is primarily caused by the $1s \rightarrow 4s$ and $1s \rightarrow 4p$ electronic transitions along with the shake-down ligand-to-metal transitions. The presence of shoulder B (8987.5 eV) caused by the splitting of the 4*p* sublevel [41–43] indicates the square coordination of the copper(II) ions in complex **I**.

The FTM EXAFS Cu *K*-edge X-ray absorption spectrum for complex **I** is shown in Fig. 3. The main peak is due to the scattering on the first coordination sphere consisting of the oxygen and nitrogen atoms of the ligand, and the peak at $r \approx 3.2$ Å is caused by

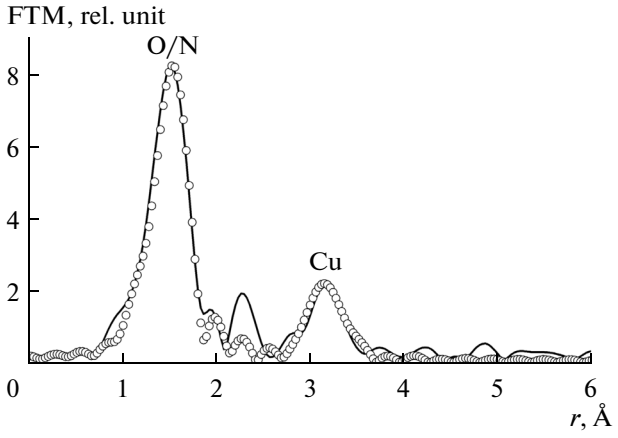

Fig. 3. FTM EXAFS Cu *K*-edge X-ray absorption spectrum of complex **I**: (solid line) experiment and (○) theoretical FTM calculated for the best model.

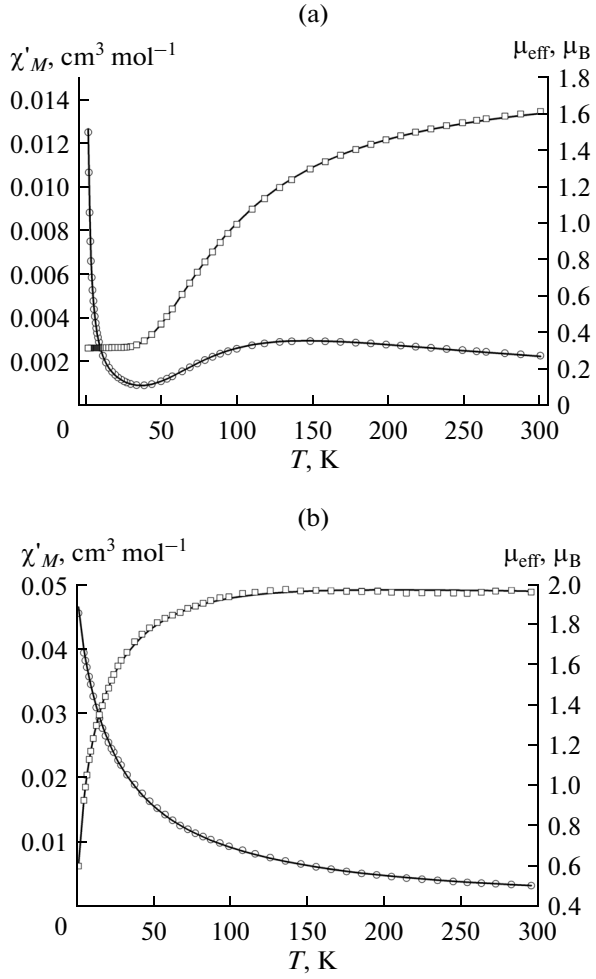

Fig. 4. Temperature dependences of χ'_M (○) and μ_{eff} (□) for complexes (left) **I** and (right) **II**; solid line is the theoretical dependence.

the scattering on the nearest copper atom, which unambiguously indicates the binuclear structure of complex **I**.

The quantitative parameters of the coordination sphere were obtained by the nonlinear multisphere fitting of the calculated EXAFS spectrum to the experimental one (Table 3). According to these parameters, the first coordination sphere of the copper ion in complex **I** is formed by the nitrogen/oxygen atoms arranged at a distance of 1.9–2.0 Å. The copper–copper distance in complex **I** (3.51 Å) considerably exceeds that for complex **II** and corresponds to the copper–copper distance in all structurally characterized acetate-bridged copper(II) complexes with bis(azomethines) based on 1,3-diaminopropan-2-ol in which the "symmetrical" conformation of the metal chelates is observed [5, 36].

The study of the temperature dependence of the magnetic susceptibility of the complexes showed a sufficiently strong exchange interaction of the opposite sign between the copper(II) ions in these complexes. The exchange interaction parameters in the complexes were calculated in the framework of the Heisenberg–Dirac–Van Vleck isotropic exchange model using the Bleaney–Bowers equation (2) [44]

$$\chi'_M = \frac{2N_A g^2\beta^2}{3kT}\left[(1-f)\times\left[1+\frac{1}{3}\exp\left(\frac{-2J}{kT}\right)\right]^{-1} + fS(S+1)\right] + N_\alpha. \quad (2)$$

Here χ'_M, N_A, g, β, k, $2J$, f, and N_α are the molar magnetic susceptibility corrected to diamagnetism of atoms, Avogadro's number, Landé factor, Bohr's magneton, exchange parameter, molar fraction of a paramagnetic impurity, and temperature-independent paramagnetism, respectively. The fixed value of N_α equal to 120×10^{-6} cm^3 mol^{-1} was used in the calculation [45].

The interdimer exchange was taken into account by Eq. (3) [45]

$$\chi_M = \frac{\chi'_M}{\left(1-\frac{2zJ'}{Ng^2\beta^2}\chi'_M\right)}. \quad (3)$$

Here χ'_M is the molar magnetic susceptibility of the dimer calculated by Eq. (2), and zJ' is the interdimer exchange parameter.

The exchange in complex **I** is antiferromagnetic. The best agreement between the theory and experiment was achieved at the following parameters of the model: $2J = -169$ cm^{-1}, $zJ' = 0$ cm^{-1}, $g = 2.11$, $f = 0.003$. The root-mean-square error R was 0.007, where

$$R = \Sigma((\chi_M^{exp} - \chi_M^{calcd})^2 / (\chi_M^{exp})^2). \quad (4)$$

The ferromagnetic exchange occurs between the copper(II) ions in complex **II** containing the μ_2-coordinated DMSO molecule (Fig. 4), and the effective magnetic moment decreases at low temperatures due to the interdimer exchange interaction of the antiferromagnetic type [45]. The best agreement between the theory and experiment is achieved at the following parameters of the model: $2J = 174$ cm^{-1}, $zJ' = -13$ cm^{-1}, $g = 2.18$, $f = 0.006$ (root-mean-square error $R = 0.022$).

The magnetic properties of complexes **I** and **II** are consistent with their structure parameters. The predominant majority of the described complexes based on *N,N*-bis(salicylidene)-1,3-diaminopropan-2-ol and its analogs with the exogenic carboxylate bridge demonstrates a fairly strong antiferromagnetic exchange (the values of $2J$ range from -100 to -200 cm^{-1}), and all of them have a "symmetrical" conformation of the binuclear fragment [5, 11, 30, 31–33]. The exchange is ferromagnetic in a few complexes of this type with the "roof-shaped" conforma-

tion [11, 35, 36–39]. The exclusion is the described [34] acetate-bridged complex based on *N,N*-bis(3-methoxy)salicylidene-1,3-diaminopropan-2-ol for which the authors give the value of exchange parameter equal to -185 cm^{-1}, while the complex, according to the X-ray diffraction data, has a "roof-shaped" conformation of the binuclear fragment (copper–copper distance 3.154(2) Å, bond angle at the alkoxyl bridging oxygen atom 107.0(2)°).

The single (up to now) case of obtaining two acetate-bridged copper(II) complexes with the same ligand, *N,N*-bis(5-*tert*-butyl-3-formylsalicylidene)-1,3-diaminopropan-2-ol, having both the "symmetrical" ($2J = -94.8$ cm^{-1}) and "roof-shaped" (with the bridging coordination of the DMSO molecule, $2J = 121$ cm^{-1}) conformations has previously been described by us [36]. Complexes **I** and **II** represent the second example showing that the character of magnetic exchange in similar systems is determined by the geometric factors rather than the nature of the exogenic bridge.

The quantum-chemical calculation of parameter $2J$ was performed in the framework of the "broken symmetry" method for the theoretical study of exchange interactions in the synthesized complexes [22–25]. The exchange parameters were calculated for both the fixed (from the X-ray diffraction data) and preliminarily optimized geometries of the complexes.

The Yamaguchi formula (5) was used for the calculation of the exchange parameter in the framework of the broken symmetry method. Formula (5) well recommended itself in combination with the hybrid functionals [25]

$$2J = \frac{2(E_{BS} - E_{HS})}{\langle S^2_{HS}\rangle - \langle S^2_{BS}\rangle}. \quad (5)$$

Here E and $\langle S^2\rangle$ are the total energy and the expected value of the squared total spin of the states, respectively; index *HS* is used to designated the high-spin state, and *BS* designates the low-spin state ("broken symmetry" state).

The calculated energies of the low- and high-spin states, exchange parameters $2J$, and values of some structure parameters for complexes **I** and **II** are listed in Table 4.

The quantum-chemical calculation of the exchange interaction parameter in complex **II** using the fixed geometry ($2J = 174$ cm^{-1}) leads to an excellent agreement with experiment. The removal of the DMSO molecule with the retained geometry (complex **I**) exerts almost no effect on the difference in energies between the triplet state and "broken symmetry" state ($2J = 180$ cm^{-1}). This indicates that the DMSO molecule is not involved in the magnetic exchange translation, which is explained by the formally orthogonal character of the magnetic orbitals of the paramagnetic centers and the axially coordinated solvent molecule [46].

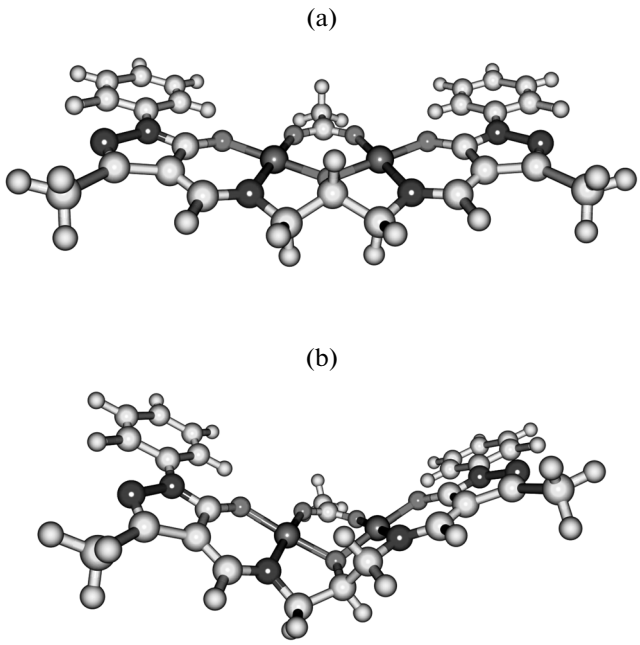

Fig. 5. Molecular structures of the (a) symmetrical and (b) distorted conformations of complex **I** according to the calculation.

The geometry optimization of complex **I** in the distorted conformation (Fig. 5) decreases the exchange parameter ($2J = 120$ cm^{-1}) but does not change its character, contradicting the experimental data on the antiferromagnetic exchange in this complex.

The total energy of the "symmetrical" conformation of complex **I** in the triplet state is by 1.39 kcal/mol lower than that of the "distorted" one. The calculated exchange parameter ($2J = -146$ cm^{-1}) in this conformation has the valid sign and also corresponds well to the experimental value ($2J = -169$ cm^{-1}). The Cu–Cu distance for this conformation (3.514 Å) is very well consistent with that obtained by the EXAFS data (3.51 Å). These results confidentially assert that the "symmetrical" conformation of the molecule of the complex takes place in the absence of the coordinated DMSO molecule.

Geometry optimization for complex **II** in the distorted conformation results in a slight flattening of the structure, and the calculated exchange parameter ($2J = 153$ cm^{-1}) agrees well with the experimental value. In the case of the symmetrical conformation of complex **II**, which is by 2.90 kcal/mol less stable than the distorted one, the triplet state is also lower than the "broken symmetry" state, and the exchange is ferromagnetic ($2J = 120$ cm^{-1}). The θ dihedral angle between the coordination planes decreases very insignificantly (Table 4) and is substantially larger than that for the distorted conformation of complex **I**.

Thus, we found the second example of "switching" the sign of the magnetic exchange from antiferromagnetic to ferromagnetic in the binuclear copper(II)

complex with bis(azomethine)-1,3-diaminopropan-2-ol due to the recrystallization of the complex from the coordinating solvent.

Based on the experimental data and quantum-chemical simulation results, we can assert that the antiferromagnetic character of exchange in complexes of this type is due to the symmetrical conformation of the binuclear fragment, while the ferromagnetic character is caused by the distorted conformation. The role of the coordinated solvent molecule as a "switch" of the exchange interaction character is only the stabilization of the distorted conformation of the metallocycles due to the axial coordination to both paramagnetic centers.

ACKNOWLEDGMENTS

This work was supported by the Russian Foundation for Basic Research, project no. 13-03-00383.

REFERENCES

1. Casellato, U., Vigato, P.A., and Vidali, M., *Coord. Chem. Rev.,* 1977, vol. 23, no. 1, p. 31.
2. Suzuki, M., Furutachi, H., and Okawa, H., *Coord. Chem. Rev.*, 2000, vols. 200–202, no. 1, p. 105.
3. Vigato, P.A. and Tamburini, S., *Coord. Chem. Rev.*, 2004, vol. 248, nos. 17–20, p. 1717.
4. Vigato, P.A., Tamburini, S., and Bertolo, L., *Coord. Chem. Rev.*, 2007, vol. 251, nos. 11–12, p. 1311.
5. Kogan, V.A., Lukov, V.V., and Shcherbakov, I.N., *Russ. J. Coord. Chem.*, 2010, vol. 36, no. 6, p. 401.
6. Mazurek, W., Kennedy, B.J., Murray, K.S., et al., *Inorg. Chem.,* 1985, vol. 24, no. 20, p. 3258.
7. Nishida, Y. and Kida, S., *Inorg. Chem.,* 1988, vol. 27, no. 3, p. 447.
8. Fallon, G.D., Markiewicz, A., Murray, K.S., and Quach, T., *J. Chem. Soc., Chem. Commun.*, 1991, no. 3, p. 198.
9. Chou, Y.-C., Huang, S.-F., Koner, R., et al., *Inorg. Chem.,* 2004, vol. 43, no. 9, p. 2759.
10. Lai, T.-C., Chen, W.-H., Lee, C.-J., et al., *J. Mol. Struct.*, 2009, vol. 935, no. 1, p. 97.
11. Kou, Y., Tian, J., Li, D., et al., *Dalton Trans.,* 2009, no. 13, p. 2374.
12. Popov, L.D., Levchenkov, S.I., Shcherbakov, I.N., et al., *Inorg. Chem. Commun.*, 2012, vol. 17, p. 1.
13. *SMART and SAINT. Release 5.0. Area Detector Control and Integration Software. Bruker AXS*, Madison (WI, USA): Analytical X-Ray Instruments, 1998.
14. Sheldrick, G.M., *SADABS. A Program for Exploiting the Redundancy of Area-detector X-Ray Data*, Göttingen (Germany): Univ. of Göttingen, 1999.
15. Sheldrick, G.M., *Acta Crystallogr., Sect. A: Found. Crystallogr.*, 2008, vol. 64, no. 1, p. 112.
16. Kochubei, D.I., Babanov, Yu.A., Zamaraev, K.I., et al., *Rentgenospektral'nyi metod izucheniya struktury amorfnykh tel: EXAFS-spektroskopiya* (X-ray Spectral Method for Structural Study of Amorphous Solids: EXAFS Spectroscopy), Novosibirsk: Nauka. Sib. otdnie, 1988.
17. Newville, M., *J. Synchrotron Rad.*, 2001, no. 8, p. 96.
18. Zabinski, S.I., Rehr, J.J., Ankudinov, A., and Alber, R.C., *Phys. Rev., B*, 1995, vol. 52, p. 2995.
19. Becke, A.D., *J. Chem. Phys.*, 1993, vol. 98, no. 7, p. 5648.
20. Lee, C., Yang, W., and Parr, R.G., *Phys. Rev. B*, 1988, vol. 37, no. 2, p. 785.
21. Popov, L.D., Shcherbakov, I.N., Levchenkov, S.I., et al., *J. Coord. Chem.*, 2008, vol. 61, no. 3, p. 392.
22. Ginsberg, A.P., *J. Am. Chem. Soc.*, 1980, vol. 102, no. 1, p. 111.
23. Noodleman, L., Peng, C.Y., Case, D.A., and Mouesca, J.-M., *Coord. Chem. Rev.*, 1995, vol. 144, p. 119.
24. Lacroix, P.G. and Daran, J.-C., *J. Chem. Soc., Dalton Trans.*, 1997, no. 8, p. 1369.
25. Soda, T., Kitagawa, Y., Onishi, T., et al., *Chem. Phys. Lett.*, 2000, vol. 319, nos. 3–4, p. 223.
26. *Gaussian 03. Revision D.01*, Wallingford (CT, USA): Gaussian, Inc., 2004.
27. Zhurko, G.A., *Chemcraft 1.6* (build 338), http://www.chemcraftprog.com
28. Kukushkin, Yu.N., Khodzhaev, O.F., Budanova, V.F., and Parpiev, N.A., *Termoliz koordinatsionnykh soedinenii* (Thermolysis of Coordination Compounds), Tashkent: Fan, 1986.
29. Kawata, T., Ohba, S., Nishida, Y., and Tokii, T., *Acta Crystallogr., Sect. C: Cryst. Struct. Commun.*, 1993, vol. 49, no. 12, p. 2070.
30. Nishida, Y. and Kida, S., *J. Chem. Soc., Dalton Trans.*, 1986, no. 12, p. 2633.
31. Weng, C.-H., Cheng, S.-C., Wei, H.-M., et al., *Inorg. Chim. Acta*, 2006, vol. 359, no. 7, p. 2029.
32. Nishida, Y., Takeuchi, M., Takahashi, K., and Kida, S., *Chem. Lett.,* 1985, vol. 14, no. 5, p. 631.
33. Kogan, V.A., Lukov, V.V., Novotortsev, V.M., et al., *Izv. Ross. Akad. Nauk, Ser. Khim.*, 2005, vol. 54, no. 3, p. 592.
34. Elmali, A., Zeyrek, C.T., and Elerman, Y., *J. Mol. Struct.*, 2004, vol. 693, nos. 1–3, p. 225.
35. Tupolova, Yu.P., Popov, L.D., Levchenkov, S.I, et al., *Russ. J. Coord. Chem.*, 2011, vol. 37, no. 7, p. 552.
36. Shcherbakov, I.N., Levchenkov, S.I., Tupolova, Yu.P., et al., *Eur. J. Inorg. Chem.,* 2013, vol. 2013, no. 28, p. 5033.
37. Lee, C.-J., Cheng, S.-C., Lin, H.-H., and Wei, H.H., *Inorg. Chem. Commun.*, 2005, vol. 8, no. 3, p. 235.
38. Dhara, K., Roy, P., Ratha, J., et al., *Polyhedron,* 2007, vol. 26, no. 15, p. 4509.
39. Chen, C.-Y., Lu, J.-W., and Wei, H.-H., *J. Chin. Chem. Soc*, 2009, vol. 56, no. 1, p. 89.
40. Yamamoto, T., *X-ray Spectrom.,* 2008, vol. 37, no. 6, p. 572.
41. Nagatani, H., Tanida, H., Watanabe, I., and Sagara, T., *Anal. Sci.,* 2009, vol. 25, no. 4, p. 475.
42. Chen, L.X., Shaw, G.B., Liu, T., et al., *Chem. Phys.,* 2004, vol. 299, nos. 2–3, p. 215.
43. Choy, J.-H., Yoon, J.-B., and Jung, H., *J. Phys. Chem. B*, 2002, vol. 106, no. 43, p. 11120.
44. Bleaney, B. and Bowers, K.D., *Proc. R. Soc. London. A,* 1952, vol. 214, no. 1119, p. 451.
45. Kahn, O., *Molecular Magnetism,* New York: VCH, 1993.
46. Queralt, N., De Graaf, C., Cabrero, J., and Caballol, R., *Mol. Phys.,* 2003, vol. 101, no. 13. p. 2095.

Translated by E. Yablonskaya